

A RADIO AND X-RAY STUDY OF HISTORICAL SUPERNOVAE IN M83

Christopher J. Stockdale¹, Larry A. Maddox², John J. Cowan², Andrea Prestwich³, Roy
Kilgard³, Stefan Immler⁴, and Miriam Krauss⁵

Received _____; accepted _____

¹Department of Physics, Marquette University, PO BOX 1881, Milwaukee, WI, 53201-1881; christopher.stockdale@marquette.edu

²Homer L. Dodge Department of Physics and Astronomy, University of Oklahoma, 440 West Brooks Room 131, Norman, OK 73019; maddox@nhn.ou.edu, cowan@nhn.ou.edu

³Harvard-Smithsonian Center for Astrophysics, 60 Garden St, Cambridge, MA, 02138; aprestwich@cfa.harvard.edu, rkilgard@cfa.harvard.edu

⁴ Exploration of the Universe Division, X-ray Astrophysics Laboratory, Code 662, NASA Goddard Space Flight Center, Greenbelt, MD 20771; immler@milkyway.gsfc.nasa.gov

⁵Department of Physics, Massachusetts Institute of Technology, Building 6-113, 77 Massachusetts Avenue, Cambridge, MA, 02139; miriam@space.mit.edu

ABSTRACT

We report the results of 15 years of radio observations of the six historical supernovae (SNe) in M83 using the Very Large Array. We note the near linear decline in radio emission from SN 1957D, a type II SN, which remains a non-thermal radio emitter. The measured flux densities from SNe 1923A and 1950B have flattened as they begin to fade below detectable limits, also type II SNe. The luminosities for these three SNe are comparable with the radio luminosities of other decades-old SNe at similar epochs. SNe 1945B, 1968L, and 1983N were not detected in the most recent observations and these non-detections are consistent with previous studies. We report the X-ray non-detections of all six historical SNe using the Chandra X-ray Observatory, consistent with previous X-ray searches of other decades-old SNe, and low inferred mass loss rates of the progenitors ($\dot{M} \approx 10^{-8} M_{\odot} \text{ yr}^{-1} [v_w/10 \text{ km s}^{-1}]$).

Subject headings: GALAXIES: INDIVIDUAL: (NGC 5236 = M83), RADIO CONTINUUM: GALAXIES, STARS: SUPERNOVAE: INDIVIDUAL (SN 1923A, SN 1945B, SN 1950B, SN 1957D, SN 1968L, SN 1983N)

1. Introduction

M83, an SABc galaxy, is a typical grand design, face-on spiral galaxy with an inclination of 24° (Talbot et al. 1979). It is relatively nearby with distance estimates ranging from 3.75 Mpc (de Vaucouleurs 1979) to 8.9 Mpc (Sandage & Tammann 1987). We have opted to use the Cepheid-established distance of 4.5 Mpc (Thim et al. 2003). The close proximity and low inclination of M83, along with six optically discovered supernovae (SNe) make it an ideal system for studying extragalactic SNe at all wavelengths. Here we report on a radio and X-ray study of six historical SNe.

Using the Very Large Array (VLA),¹ radio observations have detected emission from four historical SNe, SNe 1923A, 1950B, 1957D, and 1983N (Cowan & Branch 1982, 1985; Cowan et al. 1994; Sramek et al. 1984), while two others, SNe 1945B and 1968L have not been detected in the radio. SN 1968L lies within the bright, diffuse, radio nuclear emission and would not have been detectable unless it was extremely radio bright. This 20 year study of M83 by Cowan and collaborators has yielded an insight into the evolution of the long-term transient sources in M83, primarily SNe, supernova remnants (SNRs), and its nucleus. Chevalier (1984) proposes that synchrotron radiation is produced in the region of interaction between the SN blastwave and the circumstellar shell that originated from the prior mass loss of the progenitor star. In such models, the emission fades as the density of the circumstellar material (CSM) decreases. Cowsik & Sarkar (1984) suggest a minimum of 100 years before the radio emission re-brightens as the blastwave begins to encounter the interstellar medium, as the source evolves into a SNR. Cowan et al. (1994) charted the evolution of 14 of the brightest radio sources over the course of ten years at 6 cm and 20 cm. We have reanalyzed the Cowan et al. (1994) results and discovered at least five times

¹The VLA telescope of the National Radio Astronomy Observatory is operated by Associated Universities, Inc. under a cooperative agreement with the National Science Foundation.

the number of discrete radio sources in M83, the complete discussion will be presented in Maddox *et al.* (2005, in preparation). Immler *et al.* (1999) detected 37 discrete X-ray sources in M83 with ROSAT observations, but no radio emission was detected from the historical SNe.

In this paper we report new radio observations of the historical SNe of M83 including their current flux densities, spectral indices, and decay indices, examining how their radio emission has varied during the time that they have been monitored. We also give upper limits to the X-ray flux for the historical SNe.

2. Observations

2.1. Radio

The new VLA observations of M83 were made with four observing runs. In the first two, M83 was observed for 8.7 total hours on 13 and 15 June 1998, at 20 cm (1.450 GHz) using the VLA in its BnA configuration (the southern arms in B configuration and the northern arm in A configuration), with a maximum baseline of 24 km. During the second group of observing runs, M83 was observed on 31 October and 1 November 1998 with the VLA in its CnB configuration (maximum baseline of ~ 11 km) at 6 cm (4.860 GHz) for a total of 8.9 hours. These were done using two 25 MHz bands in dual polarization, split in 8 spectral channels each. For the purposes of this study, we are only interested in the continuum observations of the SNe and have only analyzed the Channel 0, “pseudo-continuum,” data which utilizes 75% of the 50 MHz bandwidth in each of the two orthogonal circular polarizations. The phase calibrator was J1316-336 with 3C286 used to set the flux density scale for J1316-336. In each observation, the pointing center was (J2000) $13^{\text{h}}37^{\text{m}}00^{\text{s}}22$ and $-29^{\circ}52'04''.5$.

Data were Fourier transformed and deconvolved using the CLEAN algorithm as implemented in the Astronomical Image Processing System (AIPS) routine SCIMG. The data were weighted using Briggs’s robustness parameter of 0, which minimizes the point-spread function while maximizing sensitivity. In addition, SCIMG implements a self-calibration algorithm to reduce the sidelobes from the brightest emission in the nucleus. The use of this algorithm allowed us to reduce the noise and to detect many faint sources. Uncertainties in the peak intensities are reported as the rms noise from the observations. At 20 cm, the beam size is $3''.67 \times 3''.13$, p.a. = 63.58° , and the rms noise is $0.040 \text{ mJy beam}^{-1}$. At 6 cm, the beam size is $3''.52 \times 3''.16$, p.a. = 273.0° , and the rms noise is $0.037 \text{ mJy beam}^{-1}$. The results of our analyses of the 1998 positions and peak flux densities are presented in Table 1 and Figure 1. All flux density measurements were made with the AIPS routine IMFIT using a two component model, a 2-d Gaussian component, and a linear sloping background component, which was the model used by Cowan et al. (1994). The errors reported with the flux measurements and the positions were also determined by IMFIT. The previous work of Cowan et al. (1994) and Cowan & Branch (1985) were also re-reduced and re-imaged with the same techniques used for the 1998 data. To aid in the identification and modeling of point sources, the 20 cm data taken in 1983 and 1992 were deconvolved using restoring beams similar in shape to the 1998 data (rather than the highly elliptical beams derived by SCIMG). A more detailed description of the data reduction of the earlier observations will be presented in Maddox *et al.* (2005, in preparation).

2.2. X-ray

M83 has been observed twice with Chandra using ACIS-S. The first observation was a 50ks exposure in April 2000 (ObsId 793) and the second a 10ks observation in September 2001 (ObsId 2064). These observations have been reduced as described by Kilgard et al.

(2005). No X-ray sources were detected at the positions of historical supernovae in either exposure (Soria & Wu 2002; Kilgard et al. 2005). Upper limits to the 0.3 – 8 keV X-ray luminosity are given in Table 1. The upper limits were derived from the longer observation (ObsId 793) by integrating the number of valid X-ray counts in a 5-arcsecond aperture centered on the position of the SNe. Typically 10-20 X-ray counts were obtained at each position. Since most of the counts are likely to be diffuse background intrinsic to the galaxy, the luminosities in Table 1 are hard upper limits.

3. Results & Discussion

3.1. Radio Emission from Historical Supernovae

With the VLA observations in 1998, we detect radio emission from the sites of SNe 1923A, 1950B, and 1957D at 20 cm and 6 cm, coincident, within the error limits, of the sources detected by Cowan et al. (1994) and Eck et al. (1998). No radio emission was detected from SNe 1945B, 1968L, and 1983N, and the implications of these non-detections are discussed later at the end of this Section. The measured flux densities at 20 cm and 6 cm (presented in Table 1) indicate a decrease from 1992 to 1998 for SN 1957D, but no significant changes for SNe 1923A and 1950B. SN 1957D has faded by 58% at both observed wavelengths from the prior observations in the early 1990’s.

As indicated in Table 1 (and shown in Figures 1, 2), our new observations indicate that the spectral indices (α ; $S \propto \nu^\alpha$), for both SNe 1923A and 1950B are flat. Our re-analysis of the results of Eck et al. (1998) and Cowan et al. (1994) indicate that spectral indices of both SN 1923A and SN 1950B is unchanged between the early and late 1990s. Assuming both were correctly identified as SNe, the typical model for radio emission predicts a steadily decreasing, non-thermal emission (Weiler et al. 2002). In the case of these SNe,

their radio emission is likely already at or below the level of the thermal emission from an intervening HII region along the line-of-sight (Montes et al. 1997). SN 1957D however, remains non-thermal and continues to fade at both wavelengths, as predicted by the models of Weiler et al. (1986, 1990, 2002). The evolution of these three SNe is consistent with the theoretical models of Weiler et al. (1986, 1990, 2002) and Montes et al. (1997) for radio SNe in which the 6 cm light-curve peaks before the 20 cm emission.

The observed radio properties of SNe 1923A, 1950B, and 1957D are typical of values reported for other radio SNe (See Figure 3). It is clear, for example, from Figure 3 that the inferred radio luminosities of SNe 1957D and 1950B are (at a similar age of $\simeq 30\text{--}40$ years) very similar to the luminosities of SN 1961V, in NGC 1058, and SN 1970G, in M101, at the same stage in their evolution. This correlation in luminosity also lends credence to our identification of SNe 1950B as a Type II SN. There is no reliable spectrum or optical light curve of SN 1950B to make a definitive classification as a type II SN. In particular, there has been some uncertainty in the optical position of SN 1950B that prevented a conclusive identification of the supernovae with the radio source (Cowan & Branch 1985; Cowan et al. 1994).

The evolution of the radio flux density of SNe 1923A, 1950B, and 1957D is also consistent with the current models for radio emission from SNe, which predict a general decline in radio luminosity with age and declining density of CSM. Figure 3 illustrates that trend for a number of decades-old radio SNe, with a gradual fading of the radio light curves 10 years after the supernova event. Data, fits and distances for SNe 1923A, 1950B, and 1957D are taken from this paper and Thim et al. (2003); for SN 1961V (Stockdale et al. 2001b; Silbermann et al. 1996); for SN 1968D (Hyman et al. 1995; Tully 1988); for SN 1970G (Stockdale et al. 2001a; Cowan et al. 1991; Kelson et al. 1996); for SN 1978K, (Ryder et al. 1993; Schlegel et al. 1999; Tully 1988); for SN 1979C, (Weiler et al. 1986, 1991;

Montes et al. 2000; Ferrarese et al. 1996); for SN 1980K, (Weiler et al. 1986, 1992; Montes et al. 1998; Tully 1988); for SN 1981K, (van Dyk et al. 1992; Freedman et al. 2001); for SN 1986J, (Rupen et al. 1987; Weiler et al. 1990; Silbermann et al. 1996); for SN 1987A, (Ball et al. 1995; Mitchell et al. 2001); for SN 1993J, (van Dyk et al. 1994; Freedman et al. 2001); and for Cas A and the Crab (Eck et al. 1998).

The differences in the behavior of the individual SNe are likely explained in terms of the density of the material encountered by the supernova shock. Thus, for example, the shocks associated with some radio SNe (e.g. SNe 1979C, 1970G, 1961V, and early observations of SN 1950B) might be traveling through considerably denser CSM than other similarly-aged radio SNe (e.g., SNe 1980K, 1978K, 1957D, and 1923A). Consistent with this interpretation is the very rapid decline in the radio emissions of Type Ib radio SNe, e.g. SNe 1983N and 1984L, which presumably have lower density CSM (Weiler et al. 1986; Sramek et al. 1984; Panagia et al. 1986).

One scenario which might explain an increased density of CSM around some Type II radio SNe could be that the progenitors underwent large-scale eruptions, akin to luminous blue variables (LBVs), prior to the supernova event. The mass loss rates during an LBV eruption can be 10–100× larger than the typical supergiant mass-loss rate (Humphreys & Davidson 1994). The exact epoch at which this may have occurred depends on the ejection velocities of the CSM during these events, the rate of expansion of the supernova shock, and the density of the CSM. Unfortunately these objects are too undersampled to make any definitive statements as to the exact nature of such a possible outburst or mass loss. Clearly, additional radio monitoring of SNe 1957D, 1950B, 1923A, and other radio SNe, will be important in understanding the continuing evolution and nature of these relatively rare objects.

The 1998 observations detected no radio emission from SNe 1945B, 1968L, and 1983N.

SNe 1945B and 1968L have never been detected in the radio. SN 1945B is located along a spiral arm and nothing can be inferred by its non-detection as very little is known about this SN (Liller 1990). SN 1968L is located within a region of diffuse radio emission (background level $\simeq 3$ mJy) in the nuclear region of M83. SN 1983N was detected by Cowan & Branch (1985) within 1 year after discovery with flux densities at 20cm and 6cm of 4.1 ± 0.1 mJy and 0.70 ± 0.06 mJy, the brightest historical radio SN detected in M83. SN 1983N was likely a type Ib SN and is not expected to be a detectable radio source at this epoch as type I SNe have typically very low density CSM (van Dyk et al. 1996; Weiler et al. 2002). SN 1968L would need to have been at least 3 times more luminous 15 years after explosion than SN 1983N (in the 1983 epoch) to have been detectable in the 1983 observations and in subsequent observations in the 1990’s. The diffuse nuclear radio emission coupled with the age of SN 1968L make it highly unlikely that it will ever be detected in the radio at the $1''$ resolution scale. Very long baseline interferometric (VLBI) observations have been made to study the nuclear region and search for radio emission from SN 1968L using the Long Baseline Array of the Australia Telescope National Facility. These results will be presented in a later publication.

3.2. X-ray Constraints on Historical SNe

Using the deep Chandra observation, we can put tight constraints on the X-ray emission and CSM properties of the historical SNe in M83. Assuming a thermal plasma emission with a temperature of $kT = 0.8$ keV, typical for the late emission originating in the reverse shock, the upper limits to the (0.3 – 8 keV) X-ray luminosity are a few $\times 10^{36}$ ergs s^{-1} (3σ ; see Table 1). If the CSM densities are dominated by the winds blown by the progenitor stars of the SNe, we can use the X-ray interaction luminosity $L_x = 4/[\pi m_{\text{H+He}}^2] \Lambda(T) \times (\dot{M}/v_w)^2 \times (v_s t)^{-1}$ at time t after the outburst to measure the ratio

\dot{M}/v_w (Immler & Lewin 2003). Assuming that v_w did not change over time, we can even directly estimate the mass loss rates of the progenitors.

For each of the SNe we estimate mass-loss rates of $\dot{M} \approx 10^{-8} M_\odot \text{ yr}^{-1} (v_w/10 \text{ km s}^{-1})$. Progenitors of Type II SNe following core collapse of massive stars have high mass loss rates ($\dot{M} \sim 10^{-4}$ – $10^{-6} M_\odot \text{ yr}^{-1}$) and low wind velocities of typically $v_w \sim 10 \text{ km s}^{-1}$. Type Ib/c SNe have lower mass-loss rates ($\dot{M} \sim 10^{-5}$ – $10^{-7} M_\odot \text{ yr}^{-1}$) and significantly higher wind velocities of $10 \text{ km s}^{-1} < v_w \lesssim 1,000 \text{ km s}^{-1}$.

Our inferred mass-loss rates are consistent with previous observations of other decades-old SNe. SN 1980K was reported with an X-ray luminosity of $3.1 \times 10^{37} \text{ erg s}^{-1}$ measured with ROSAT in 1992 in the 0.1 – 2.4 keV range and was not detected in Chandra observations in 2001 with a limiting detection threshold of $\sim 10^{37} \text{ erg s}^{-1}$ in the 0.3 – 5 keV range (Schlegel 1994; Holt et al. 2003). There have been numerous X-ray SNe detected with $L_X \sim 10^{38}$ – $10^{41} \text{ erg s}^{-1}$ and there has been a clear correlation between their X-ray and radio luminosities in the first ten years following the SN explosion (Pooley et al. 2002). No X-ray emission has been detected from SNe with ages comparable to those of SNe 1957D, 1950B, and 1923A, with upper limits established for SNe 1959D (in NGC 7331) of $1.2 \times 10^{38} \text{ erg s}^{-1}$ and 1961V (in NGC 1058) of $1.5 \times 10^{40} \text{ erg s}^{-1}$ (Stockdale et al. 1998b,a).

Each X-ray observation at time t is related to the corresponding distance r from the site of the explosion, $r = v_s \times t$ (with shock front velocity v_s), and to the age of the stellar wind, $t_w = tv_s/v_w$. The Chandra measurements decades after the outbursts of the historical SNe in M83 probe the CSM at large radii ($> 10^{18} \text{ cm}$) from the sites of the explosions. The observed lack of significant X-ray emission is due to the lack of shocked CSM originating in the low-density stellar winds of the progenitors.

4. Summary

M83 serves as an excellent laboratory to study decades-old SNe as they transition into SNRs. The 15 year study by Cowan and collaborators has provided valuable insight into the evolution of these historical SNe and the nature of the environment. We report the continued decline in the non-thermal radio emission from SN 1957D and the apparent fading of SN 1923A and 1950B below the confusion level of associated or intervening HII regions. We further report that SN 1983N was not detected in the latter epochs since its initial discovery in 1983 and its behavior is typical of type Ib and Ic SNe. The radio non-detections of SNe 1945B and 1968L are also noted, although very little can be inferred from these results due to lack of information about these sources and (in the case of SN 1968L) strong diffuse emission in the nuclear region of M83. Finally, we report the X-ray non-detection of all six historical SNe with Chandra. These results place more stringent constraints on the mass-loss rates of the progenitors than was previously possible. VLA observations are needed to explore the radio emission in these decades-old SNe and to continue to chart their evolution from SNe into SNRs.

We thank Michael P. Rupen for his assistance in imaging the 20 cm 1998 VLA data, Christina Lacey who was the Principle Investigator for the 1998 radio observations, and Emily Wolfing for her contributions through the NSF/REU program at the University of Oklahoma. We also express our appreciation to an anonymous referee, whose comments were very useful in improving this manuscript. The research was supported in part by the NSF (AST-0307279 to JJC), Chandra (GO1-2092B), the NASA Wisconsin Space Grant Consortium (CJS), and by an award from Research Corporation (C. Stockdale is a Cottrell Scholar). We have made use of the NASA/IPAC Extragalactic Database (NED), which is operated by the Jet Propulsion Laboratory, Caltech, under contract with the National Aeronautics and Space Administration, and have made use of the new NRAO Data Archival

Service.

REFERENCES

- Ball, L., Campbell-Wilson, D., Crawford, D. F., & Turtle, A. J. 1995, *ApJ*, 453, 864
- Chevalier, R. A. 1984, *ApJ*, 285, L63
- Cowan, J. J., & Branch, D. 1982, *ApJ*, 258, 31
- . 1985, *ApJ*, 293, 400
- Cowan, J. J., Goss, W. M., & Sramek, R. A. 1991, *ApJ*, 379, L49
- Cowan, J. J., Roberts, D. A., & Branch, D. 1994, *ApJ*, 434, 128
- Cowsik, R., & Sarkar, S. 1984, *MNRAS*, 207, 745
- de Vaucouleurs, G. 1979, *AJ*, 84, 1270
- Eck, C. R., Roberts, D. A., Cowan, J. J., & Branch, D. 1998, *ApJ*, 508, 664
- Ferrarese, L., Freedman, W. L., Hill, R. J., Saha, A., Madore, B. F., Kennicutt, R. C., Stetson, P. B., Ford, H. C., Graham, J. A., Hoessel, J. G., Han, M., Huchra, J., Hughes, S. M., Illingworth, G. D., Kelson, D., Mould, J. R., Phelps, R., Silbermann, N. A., Sakai, S., Turner, A., Harding, P., & Bresolin, F. 1996, *ApJ*, 464, 568
- Freedman, W. L., Madore, B. F., Gibson, B. K., Ferrarese, L., Kelson, D. D., Sakai, S., Mould, J. R., Kennicutt, R. C., Ford, H. C., Graham, J. A., Huchra, J. P., Hughes, S. M. G., Illingworth, G. D., Macri, L. M., & Stetson, P. B. 2001, *ApJ*, 553, 47
- Holt, S. S., Schlegel, E. M., Hwang, U., & Petre, R. 2003, *ApJ*, 588, 792
- Humphreys, R. M., & Davidson, K. 1994, *PASP*, 106, 1025
- Hyman, S. D., van Dyk, S. D., Weiler, K. W., & Sramek, R. A. 1995, *ApJ*, 443, L77

- Immler, S., Vogler, A., Ehle, M., & Pietsch, W. 1999, *A&A*, 352, 415
- Immler, S., & Lewin, W. H. G. 2003, *Lecture Notes in Physics*, Berlin Springer Verlag, 598, 91
- Kelson, D. D., Illingworth, G. D., Freedman, W. F., Graham, J. A., Hill, R., Madore, B. F., Saha, A., Stetson, P. B., Kennicutt, R. C., Mould, J. R., Hughes, S. M., Ferrarese, L., Phelps, R., Turner, A., Cook, K. H., Ford, H., Hoessel, J. G., & Huchra, J. 1996, *ApJ*, 463, 26
- Kilgard, R. E., Cowan, J. J., Garcia, M. R., Kaaret, P., Krauss, M. I., McDowell, J. C., Prestwich, A. H., Primini, F. A., Stockdale, C. J., Trinchieri, G., Ward, M. J., & Zezas, A. 2005, *ApJS*, 159, 214
- Liller, W. 1990, *IAU Circ.*, 5091, 2
- Mitchell, R. C., Baron, E., Branch, D., Lundqvist, P., Blinnikov, S., Hauschildt, P. H., & Pun, C. S. J. 2001, *ApJ*, 556, 979
- Montes, M. J., Weiler, K. W., & Panagia, N. 1997, *ApJ*, 488, 792
- Montes, M. J., van Dyk, S. D., Weiler, K. W., Sramek, R. A., & Panagia, N. 1998, *ApJ*, 506, 874
- Montes, M. J., Weiler, K. W., Van Dyk, S. D., Panagia, N., Lacey, C. K., Sramek, R. A., & Park, R. 2000, *ApJ*, 532, 1124
- Panagia, N., Sramek, R. A., & Weiler, K. W. 1986, *ApJ*, 300, L55
- Pooley, D., Lewin, W. H. G., Fox, D. W., Miller, J. M., Lacey, C. K., Van Dyk, S. D., Weiler, K. W., Sramek, R. A., Filippenko, A. V., Leonard, D. C., Immler, S., Chevalier, R. A., Fabian, A. C., Fransson, C., & Nomoto, K. 2002, *ApJ*, 572, 932

- Rupen, M. P., van Gorkom, J. H., Knapp, G. R., Gunn, J. E., & Schneider, D. P. 1987, *AJ*, 94, 61
- Ryder, S., Staveley-Smith, L., Dopita, M., Petre, R., Colbert, E., Malin, D., & Schlegel, E. 1993, *ApJ*, 416, 167
- Sandage, A., & Tammann, G. A. 1987, *A revised Shapley-Ames Catalog of bright galaxies* (Carnegie Institution of Washington Publication, Washington: Carnegie Institution, 1987, 2nd ed.)
- Schlegel, E. M. 1994, *AJ*, 108, 1893
- Schlegel, E. M., Ryder, S., Staveley-Smith, L., Petre, R., Colbert, E., Dopita, M., & Campbell-Wilson, D. 1999, *AJ*, 118, 2689
- Silbermann, N. A., Harding, P., Madore, B. F., Kennicutt, R. C., Saha, A., Stetson, P. B., Freedman, W. L., Mould, J. R., Graham, J. A., Hill, R. J., Turner, A., Bresolin, F., Ferrarese, L., Ford, H., Hoessel, J. G., Han, M., Huchra, J., Hughes, S. M. G., Illingworth, G. D., Phelps, R., & Sakai, S. 1996, *ApJ*, 470, 1
- Soria, R., & Wu, K. 2002, *A&A*, 384, 99
- Sramek, R. A., Panagia, N., & Weiler, K. W. 1984, *ApJ*, 285, L59
- Stockdale, C. J., Cowan, J. J., & Romanishin, W. 1998a, *Bulletin of the American Astronomical Society*, 30, 1260
- Stockdale, C. J., Romanishin, W., & Cowan, J. J. 1998b, *ApJ*, 508, L33
- Stockdale, C. J., Goss, W. M., Cowan, J. J., & Sramek, R. A. 2001a, *ApJ*, 559, L139
- Stockdale, C. J., Rupen, M. P., Cowan, J. J., Chu, Y., & Jones, S. S. 2001b, *AJ*, 122, 283

- Talbot, R. J., Jensen, E. B., & Dufour, R. J. 1979, *ApJ*, 229, 91
- Thim, F., Tammann, G. A., Saha, A., Dolphin, A., Sandage, A., Tolstoy, E., & Labhardt, L. 2003, *ApJ*, 590, 256
- Tully, R. B. 1988, *Nearby galaxies catalog* (Cambridge and New York, Cambridge University Press, 1988, 221 p.)
- van Dyk, S. D., Weiler, K. W., Sramek, R. A., & Panagia, N. 1992, *ApJ*, 396, 195
- van Dyk, S. D., Weiler, K. W., Sramek, R. A., Rupen, M. P., & Panagia, N. 1994, *ApJ*, 432, L115
- van Dyk, S. D., Hamuy, M., & Filippenko, A. V. 1996, *AJ*, 111, 2017
- Weiler, K. W., Sramek, R. A., Panagia, N., van der Hulst, J. M., & Salvati, M. 1986, *ApJ*, 301, 790
- Weiler, K. W., Panagia, N., & Sramek, R. A. 1990, *ApJ*, 364, 611
- Weiler, K. W., van Dyk, S. D., Discenna, J. L., Panagia, N., & Sramek, R. A. 1991, *ApJ*, 380, 161
- Weiler, K. W., van Dyk, S. D., Panagia, N., & Sramek, R. A. 1992, *ApJ*, 398, 248
- Weiler, K. W., Panagia, N., Montes, M. J., & Sramek, R. A. 2002, *ARA&A*, 40, 387

Table 1. Radio flux densities and upper limits to the X-ray luminosity for historical SNe in M83. Note: 1

mJy = 2.41×10^{25} erg s⁻¹ Hz⁻¹ at a distance of 4.5 Mpc (Thim et al. 2003). ^a

Source	Position		1998 Flux Densities			1990 – 1992 Flux Densities			L _X (0.3 – 8 keV)
	RA	Dec	20cm	6cm	Spectral	20cm	6cm	Spectral	3 σ upper limit
SN	(J2000)	(J2000)	(mJy)	(mJy)	Index	(mJy)	(mJy)	Index	(ergs s ⁻¹)
1957D	13 ^h 37 ^m 03 ^s 57	-29°49'40''6	0.73 ± 0.09	0.64 ± 0.05	-0.11 ± 0.15	1.75 ± 0.07	1.50 ± 0.04	-0.13 ± 0.06	2.2 × 10 ³⁶
1950B	13 ^h 36 ^m 52 ^s 08	-29°51'55''7	0.50 ± 0.05	0.47 ± 0.04	-0.05 ± 0.13	0.52 ± 0.05	0.49 ± 0.04	-0.05 ± 0.13	1.4 × 10 ³⁶
1923A	13 ^h 37 ^m 09 ^s 31	-29°51'00''7	≤ 0.15	0.21 ± 0.04	≥ +0.28	0.17 ± 0.05	0.21 ± 0.03	+0.18 ± 0.33	2.2 × 10 ³⁶
1983N	13 ^h 36 ^m 50 ^s 31	-29°54'02''3	≤ 0.15	≤ 0.12	1.7 × 10 ³⁶
1945B	13 ^h 36 ^m 51 ^s	-30°10'17''	≤ 0.15	≤ 0.12	3.6 × 10 ³⁶

^aSN 1968L is located in the confused nuclear region of the galaxy. We were unable to get meaningful limits for either radio or X-ray luminosities.

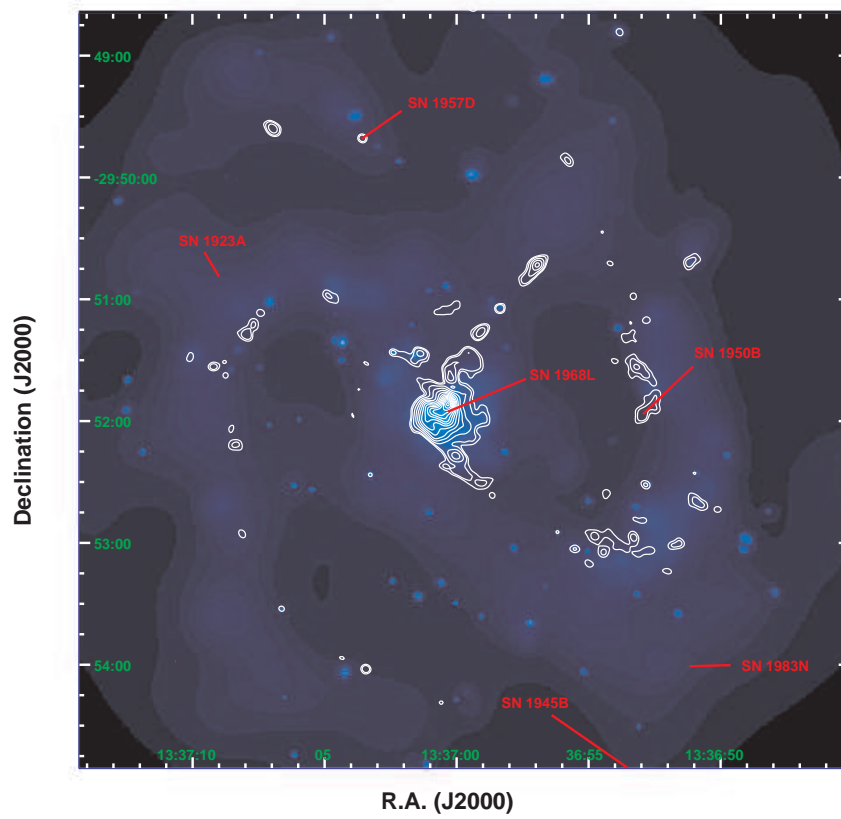


Fig. 1.— Radio contours (20 cm; 1998) overlaying the soft X-ray (0.3 – 2 keV; 2001) image of M83.

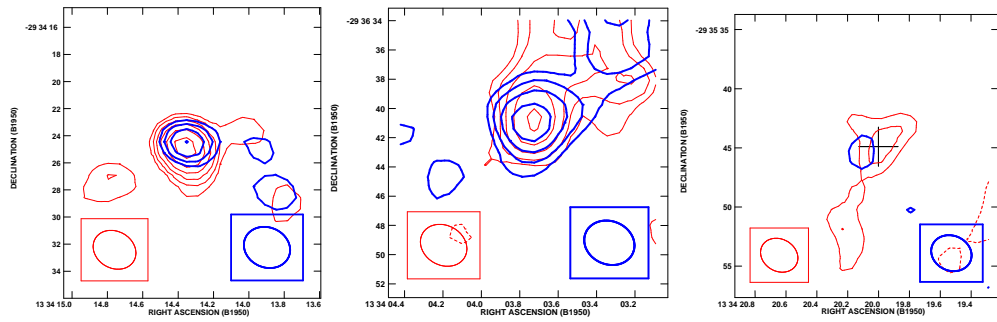


Fig. 2.— Radio contour images at 20 cm (in red) and 6 cm (in blue) of SNe 1957D, 1950B, and 1923A (from left to right). Contour levels at both wavelengths are $-0.12, 0.12, 0.17, 0.24, 0.34, 0.48, 0.68,$ and $0.96 \text{ mJy beam}^{-1}$. At 20 cm, the beam size is shown in the lower left, and at 6 cm, the beam size is shown in the lower right.

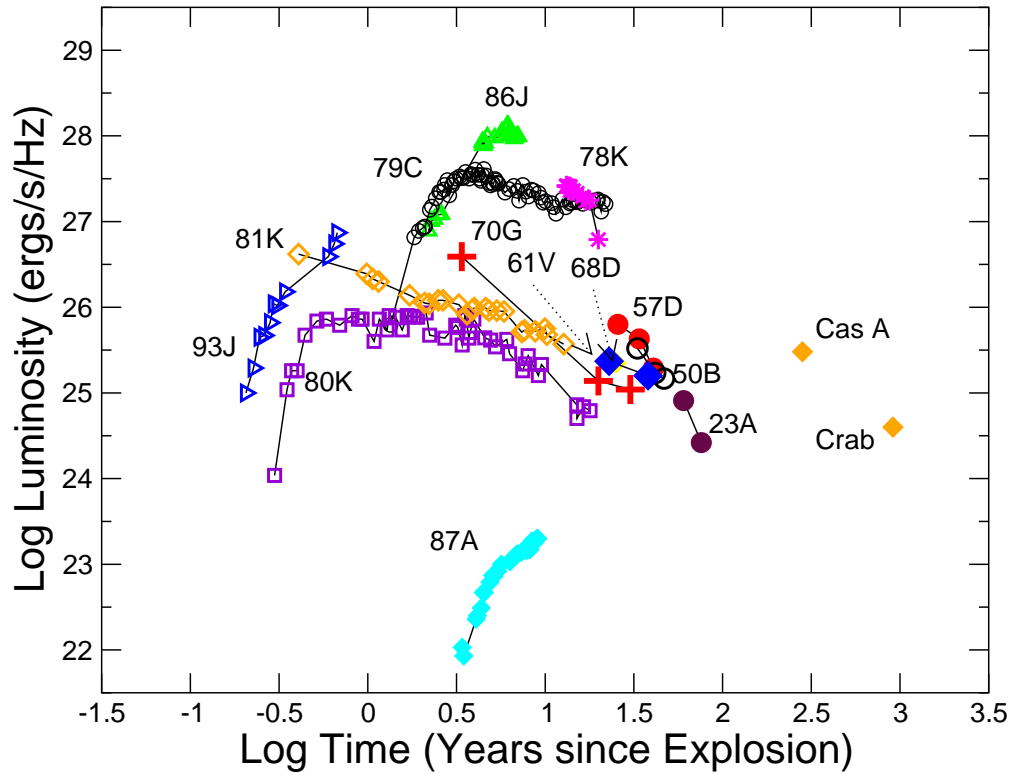


Fig. 3.— 20 cm radio light curve of several radio SNe II and SNRs. Data and distances for SNe 1923A (maroon filled circle and maroon, open, inverted triangle for upper limit), 1950B (black open circles) & 1957D (red filled circles); for SN 1961V (blue filled diamonds); for SN 1968D (yellow filled diamond); SN 1970G (red crosses); for SN 1978K (magenta stars); for SN 1979C (black open circles); for SN 1980K (purple open boxes); for SN 1981K (orange open diamonds); for SN 1986J (green triangles); for SN 1987A (cyan filled diamonds); and for SN 1993J (blue open triangles). Luminosities for Cas A and the Crab (orange filled diamonds).